◆ Human Brain Mapping 31:126–139 (2010) ◆

Specialization in the Default Mode: Task-Induced Brain Deactivations Dissociate Between Visual Working Memory and Attention

Jutta S. Mayer,[1]* Alard Roebroeck,[2] Konrad Maurer,[1] and David E.J. Linden[3]

[1]*Department of Psychiatry, Goethe-University, 60528 Frankfurt, Germany*
[2]*Faculty of Psychology and Neuroscience, Department of Cognitive Neuroscience, University of Maastricht, 6200 MD Maastricht, The Netherlands*
[3]*School of Psychology, University of Wales Bangor, Bangor LL57 2AS, United Kingdom*

Abstract: The idea of an organized mode of brain function that is present as default state and suspended during goal-directed behaviors has recently gained much interest in the study of human brain function. The default mode hypothesis is based on the repeated observation that certain brain areas show task-induced deactivations across a wide range of cognitive tasks. In this event-related functional resonance imaging study we tested the default mode hypothesis by comparing common and selective patterns of BOLD deactivation in response to the demands on visual attention and working memory (WM) that were independently modulated within one task. The results revealed task-induced deactivations within regions of the default mode network (DMN) with a segregation of areas that were additively deactivated by an increase in the demands on both attention and WM, and areas that were selectively deactivated by either high attentional demand or WM load. Attention-selective deactivations appeared in the left ventrolateral and medial prefrontal cortex and the left lateral temporal cortex. Conversely, WM-selective deactivations were found predominantly in the right hemisphere including the medial-parietal, the lateral temporo-parietal, and the medial prefrontal cortex. Moreover, during WM encoding deactivated regions showed task-specific functional connectivity. These findings demonstrate that task-induced deactivations within parts of the DMN depend on the specific characteristics of the attention and WM components of the task. The DMN can thus be subdivided into a set of brain regions that deactivate indiscriminately in response to cognitive demand ("the core DMN") and a part whose deactivation depends on the specific task. *Hum Brain Mapp 31:126–139, 2010.* © 2009 Wiley-Liss, Inc.

Key words: working memory; visual attention; default mode; deactivation; fMRI

Additional Supporting Information may be found in the online version of this article.

Contract grant sponsor: Wellcome Trust; Contract grant number: 077185/Z/05/Z; Contract grant sponsor: German Ministry for Education and Research/German Research Council; Contract grant number: DLR 01GO0203; Contract grant sponsor: German Research Council.

*Correspondence to: Jutta S. Mayer, PhD, Department of Psychiatry, Goethe-University, Heinrich-Hoffmann-Str. 10, 60528 Frankfurt, Germany. E-mail: jutta.mayer@kgu.de

Received for publication 22 December 2008; Revised 8 May 2009; Accepted 7 June 2009

DOI: 10.1002/hbm.20850

Published online 28 July 2009 in Wiley InterScience (www.interscience.wiley.com).

INTRODUCTION

The functional significance of the "default mode" of brain activity [Gusnard and Raichle, 2001; Raichle et al., 2001] and the neural processes involved in its deactivation during cognitive tasks are central topics in the study of human brain function [Bar et al., 2007; Mason et al., 2007; McKiernan et al., 2006]. The default mode network (DMN) has been identified as a set of brain regions that typically have higher signal levels at rest or a cognitively simple baseline task compared to a more demanding experimental task. In the standard analysis of functional imaging data that is based on signal changes compared to a baseline, these regions would thus show a task-induced deactivation. The DMN typically comprises regions in the medial prefrontal cortex (PFC) [ventromedial PFC, anterior cingulate cortex (ACC)], the medial parietal cortex [posterior cingulate cortex (PCC), precuneus, retrosplenial cortex], and lateral temporo-parietal cortex [supramarginal gyrus (SMG), angular gyrus, superior temporal sulcus]. These regions have consistently shown task-induced deactivations across participants and across a wide variety of cognitive tasks (e.g., attention, memory, language processing, and motor tasks) [Binder et al., 1999; Mazoyer et al., 2001; Shulman et al., 1997]. This suggests that task-induced deactivations are independent of the characteristics of the task. Moreover, task-induced deactivations are related to task-demands. Increasing working memory (WM) load or the demands on visual attention for target detection leads to an increase in blood oxygen-level-dependent (BOLD) deactivation [McKiernan et al., 2003, 2006; Todd et al., 2005; Tomasi et al., 2007]. This finding has led to the assumption that default activity is an inverse function of cognitive demand, where higher demands reduce activity in the default regions because the mental resources used for various internal processes are suspended to accommodate task-related processing [Gusnard and Raichle, 2001; McKiernan et al., 2003, 2006; Raichle et al., 2001].

Although the default mode theory has recently gained much interest, caution should be used in interpreting task-induced deactivations in terms of the disengagement of specific cognitive processes. The relationship between neuronal activity and the negative BOLD response, which depends on the complex interplay between hemodynamics and metabolism, is still unclear. Support for a neuronal [Shmuel et al., 2006] rather than hemodynamic origin [Harel et al., 2002] for the negative BOLD response has been demonstrated. However, a sustained negative BOLD signal does not necessarily imply decreased neuronal activity but in some circumstances can also result from increased neuronal activity [Schridde et al., 2008].

Recent functional magnetic resonance imaging (fMRI) studies on WM and attention that successfully exploit the effects of BOLD deactivation on behavioral performance have challenged the default mode theory as well [Hampson et al., 2006; Shulman et al., 2003, 2007]. For instance, when subjects monitored a stream of distracter objects for a target, the BOLD deactivation preceding the target in the right temporal-parietal junction was found to be stronger on trials in which the target was detected than missed. This finding has been interpreted in terms of filtering of distracting information rather than the disengagement of task-independent processes [Shulman et al., 2007]. Assessing functional connectivity between cortical regions at rest has become a prominent approach in the study of the DMN. Hampson et al. [2006] studied functional connectivity between nodes in the DMN at rest and during the performance of a WM task. Consistent with previous studies [Fox et al., 2005; Greicius et al., 2003], they demonstrated that the PCC and portions of the medial frontal gyrus and ventral ACC were functionally connected at rest. However, in contradiction to the default mode theory, functional connectivity between the two regions was also found during a verbal WM task and positively correlated with WM performance. Taken together, these findings suggest that deactivations in some default mode regions during WM and attention tasks depend on the characteristics of the task and have functional significance for the performance of specific tasks.

The present fMRI study aimed at testing the default mode theory by comparing common and selective patterns of BOLD deactivation in response to the demands on visual attention and WM. The task combined visual search and delayed discrimination of complex objects and the demands on selective attention and WM encoding were modulated independently [Mayer et al., 2007a,b]. On each trial participants were presented with a search array and performed easy visual search (ES, = low attentional demand) or difficult visual search (DS, = high attentional demand) to encode one (WM Load 1) or three (WM Load 3) complex objects into WM (see Fig. 1). This design allowed direct testing for common and differential effects of visual attention and WM that were not confounded by the differences in sensory stimulation, scanning parameters, and subject sample that complicate comparisons across experiments. The common and differential effects of visual attention and WM encoding were investigated in terms of task-induced deactivation and brain connectivity.

According to the default mode theory we predicted decreasing BOLD signal as a function of task demand in a highly similar set of regions for both the attention and WM components of the task. In these overlap areas we expected an additive increase in BOLD deactivation as a consequence of an increase in the demand on WM and visual search difficulty. The default mode theory would also predict that during execution of the task regions of deactivation should not show task-specific functional connectivity because their decreased engagement would be task-independent.

In contrast, if an increase in the demands on selective attention and WM encoding resulted in increased BOLD deactivation at different cortical sites, it would suggest that decreases in BOLD activity are dependent on the characteristics of each task component. This would be

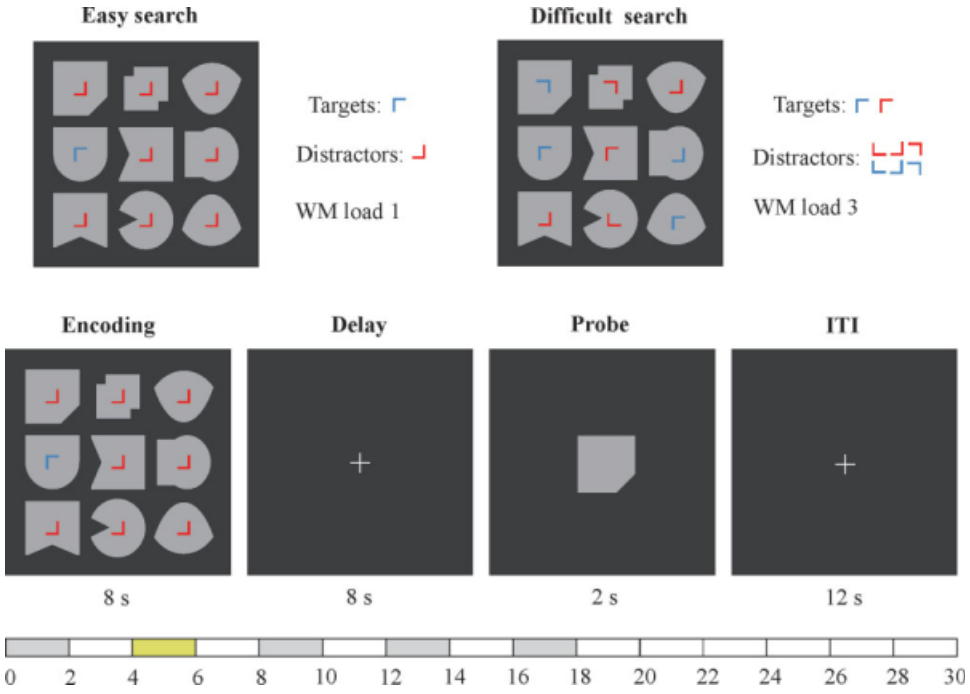

Figure 1.

Stimuli and trial design. Participants were presented with a search array and asked to memorize only the objects marked with a target item. The targets were either easy to discriminate from the distractors ("easy search") or not ("difficult search"). WM load was manipulated by changing the number of targets (Load 1, left array; Load 3, right array). The search array was presented for 8 s and the analysis focused on the late encoding predictor (green bar, grey: additional predictors). ITI: intertrial interval.

inconsistent with a model of suppression of a common network under increasing cognitive demand. In this case we would also expect functional connectivity between regions of deactivation during task execution with spatially segregated patterns for visual attention and WM.

MATERIALS AND METHODS

The current analysis was based on data from a previously published experiment [Mayer et al., 2007b].

Subjects

About 18 healthy participants (9 females, mean age 28.2 ± 6.6, range: 20–44), who reported normal or corrected-to-normal visual acuity, normal color vision, and no history of neurological or psychiatric illness, participated. The study was approved by the local ethics committee. All participants gave written informed consent.

Stimuli, Task, and Procedure

Each participant was presented with a search array and performed easy or difficult visual search to encode one or three complex objects into WM. The display in the study phase consisted of nine different grey geometric shapes (each spanning ~1.1° × 1.1° of visual angle), arranged in a 3 × 3 matrix, and presented in the center of the screen and on a black background. The shapes were selected at random without replacement from a set of 12 shapes and each was oriented randomly in one of the four possible directions, having to discriminate, in total, between 48 different objects. In the center of each shape we placed a small L-shaped item (0.3° × 0.3°). The Ls appeared in one of four different orientations (0°, 90°, 180°, and 270°, clockwise) and were colored either blue or red. Each 30-s trial began with the presentation of the search array for 8 s. Participants needed to memorize only the objects marked with an L in 90° orientation (target items). The objects associated with Ls of other orientations could be ignored (distractor items). In the easy search condition target L's always appeared in blue and distractors in red. Distractor L's were always oriented 270°. In the difficult search condition each target and distractor was assigned randomly either blue or red color. In this condition, the distractor items could take any of the remaining three orientations (0°, 180°, and 270°). The search array contained either one or three targets (WM Load 1 and 3). After an 8-s delay interval, a probe that consisted of a single object appeared

for 2 s at the center position of the array. Participants responded with a left- or right-hand button press to indicate whether the probe did or did not match in the form and orientation one of the memorized objects. Half of the trials were matches. The intertrial interval lasted 12 s. Each fMRI run (four runs per session) included six iterations of each of the four trial types (Load 1/ES; Load 3/ES; Load 1/DS; Load 3/DS). We presented easy and difficult search conditions in separate blocks of six trials (two blocks for each condition per run) in a pseudo-randomized order across runs. WM load conditions were fully randomized within each block.

Image Acquisition and Analysis

Anatomical three-dimensional T1-weighted images and functional images were acquired on a 3 T Magnetom Trio scanner (Siemens Medical Systems, Erlangen, Germany) equipped with a standard head coil. Functional images were collected using 34 slices (3 mm thickness with 3.4 × 3.4 mm^2 in-plane resolution) covering the whole brain with a BOLD-sensitive echo-planar imaging sequence (repetition time = 2 s, echo time = 30 ms, flip angle = 80°; matrix = 64 × 64; duration of each run = 780 s).

Image analyses were performed with Brainvoyager QX, version 1.4.9 (Brain Innovation, Maastricht, The Netherlands). Data preprocessing included slice scan time correction with the first scan time within a volume used as a reference for alignment by sinc interpolation, three-dimensional motion correction, spatial smoothing with an 8-mm Gaussian kernel (full width at half-maximum), temporal high pass filtering with a cut-off of 260 s to remove low-frequency nonlinear drifts of three or fewer cycles per time course, and linear trend removal. Talairach transformation was performed for the complete set of functional data of each participant, yielding a 4-D data representation (volume time course: 3 × space, 1 × time). A multisubject statistical analysis was performed by multiple linear regression of the BOLD response time course in each voxel. The general linear model of the experiment was computed for 72 z-normalized volume time courses (18 participants × 4 runs). For each of the four experimental conditions, five task phases were defined representing early encoding (0–4 s) and late encoding (4–8 s), early delay (8–12 s), late delay (12–16 s), and retrieval (16–18 s). The different task phases were modeled by predictors of 2-s duration to avoid contamination by variance in the fMRI signal attributable to neural activity that occurred in the preceding or subsequent task phases [Zarahn et al., 1997]. The signal values during these phases were considered the effects of interest. The corresponding predictors were obtained by convolution of an ideal box-car response with a gamma function model of the hemodynamic response [Friston et al., 1998]. All error trials were collapsed on a separate predictor. Activation during the intertrial interval (12 s) served as experimental baseline. In addition, we computed two models that coded each experimental condition across the whole encoding phase (0–8 s after stimulus onset). One model also included separate predictors for the delay and retrieval phases as introduced above (Model no. 1) whereas the other model only included the encoding predictor (Model no. 2). A further model was included that coded each experimental condition across the whole trial (0–18 s after stimulus onset) (Model no. 3) (see Supporting Information Fig. 1A).

The 3D group statistical maps were generated by associating each voxel with the *F*-value corresponding to the specific set of predictors and calculated on the basis of the least mean squares solution of the general linear model with a random-effects model. The obtained beta weights of each predictor served as input for the second-level whole-brain random-effects analysis including a 2 × 2 factorial design (Factor 1: attention, Level 1: ES, Level 2: DS; Factor 2: WM load, Level 1: Load 1, Level 2: Load 3). Main and interaction effects were tested based on F-statistics. To compare activations and deactivations between experimental conditions within one task phase, linear contrasts were performed using t-statistics.

Deactivations were first analyzed across experimental conditions by contrasting BOLD activity during the late encoding phase (ES1/late encoding + ES3/late encoding + DS1/late encoding + DS3/late encoding) against baseline activity. We then tested whether these deactivations were modulated by the demands on attention and/or WM load in the following way: first, three separate masks were defined based on the group statistical maps that reflected a significant main effect of attentional demand, WM load, and the interaction between the two factors, thus including both regions of activations and deactivations. Second, the GLM was calculated separately for each mask. The design matrix was the same as for the whole brain analysis, but the GLM was restricted to the voxels of the functionally defined masks. Significant decreases from baseline were then extracted by contrasting BOLD activity during the late encoding phase (ES1/late encoding + ES3/late encoding + DS1/late encoding + DS3/late encoding) against baseline activity. Multisubject statistical maps were thresholded at $q < 0.05$, corrected for false discovery rate [Genovese et al., 2002] and visualized on a surface reconstruction of the MNI template brain (courtesy of the Montreal Neurological Institute).

FMRI time courses were shown for selected ROIs where the effects of WM load and attentional demand appeared most prominently. The ROIs were functionally defined based on the multisubject statistical volume maps. Starting from the voxel showing peak activation in the multisubject map, a cuboid with a total volume of 216 mm^3 each was marked. Representative time courses for each experimental condition were obtained by averaging the percent signal changes of the individual voxels within the obtained volume across all participants and repetitions.

Additionally, the specificity of regional differences in deactivation was tested (i) within those regions that

showed a significant effect of WM load, attentional demand, or both in the present task and (ii) within regions of the DMN as described previously [Shulman et al., 1997]. The coordinates from Table I and the study of Shulman et al. [1997] were chosen to define the centers of ROIs that comprised a cuboid with a total volume of 216 mm^3 each. The contrast DS1/late encoding—ES3/late encoding was calculated within these ROIs. This contrast allowed us to identify regions where activation in response to high attentional demand was stronger than activation related to high WM load and vice versa which would be taken as evidence for differential deactivation associated with WM load or attentional demand.

Granger causality mapping (GCM) [Goebel et al., 2003; Roebroeck et al., 2005] was applied to investigate functional connectivity between regions of task-induced deactivation. The basic idea of this method is to use temporal information in stochastic time series of a brain region ($X[t]$) to predict signal time courses in other brain regions ($Y[t]$). According to this method instantaneous influence (nondirected correlation) between X and Y is said to exist when values $X[t]$ improve predictions of contemporaneous values $Y[t]$ (or vice versa) taking into account the predictive value of past values of those same regional time series. Vector autoregressive modeling can be used to apply this definition to fMRI time-series [Roebroeck et al., 2005]. GCMs with an autoregression order of 1 were computed from signal time courses to estimate the instantaneous influence between the voxels of selected ROIs (left superior frontal gyrus [SFG] and right SMG) and all other voxels in the scanned volume. As our primary interest was on the encoding phase the signal time courses included only the first 6 volumes of each trial. The ROIs were functionally defined based on the multisubject GLM. Peak activation for the attention and WM contrasts defined the centers of two ROIs that showed consistent patterns of deactivation across the three different models that coded the encoding phase separately: the left SFG, which was selectively responsive to increased attentional demand and the right SMG, which was selectively responsive to increased WM load. Each ROI comprised a cuboid with a total volume of 1,000 mm^3 each. The time course averaged across voxels of a ROI was taken as a reference and the instantaneous influence was computed for each subject including all conditions. The instantaneous influence values for each subject were then entered into a second-level multisubject analysis with a random effects model. We compared differences in instantaneous influence values between the left SFG and the right SMG based on t-statistics. To correct for multiple comparisons we performed a cluster-size thresholding [Forman et al., 1995] that makes use of a Monte Carlo simulation (1,000 iterations). Thus, the difference map was thresholded at $P = 0.05$, corrected for multiple comparisons. The individual maps were thresholded at $P = 0.01$, corrected for multiple comparisons.

TABLE I. Brain regions showing significant deactivations in the contrasts for encoding

Brain region	BA	x	y	z
WM-selective				
R anterior cingulate	42	6	41	7
L medial FG	10	−7	54	13
R medial FG	9	4	47	29
R IFG	46	45	39	3
L STG	38	−43	12	−18
R MTG	22	66	−31	4
R SMG	40	51	−54	34
R precuneus	31	7	−50	30
R posterior cingulate	31	12	−43	35
Attention-selective				
L anterior cingulate	24	−8	32	−3
L medial FG	6	−4	−18	48
R medial FG	9	5	37	31
L paracentral lobule	31	−5	−30	47
R paracentral lobule	6	8	−24	46
L SFG	9	−8	50	36
L IFG	47	−37	29	−6
R insula	13	50	−33	18
L STG	42	−58	−27	14
R STG	22	51	−10	9
L MTG	21	−58	−18	−7
L angular gyrus	39	−41	−65	36
L globus pallidus		−16	−10	−7
R globus pallidus		25	−12	−7
Common deactivation				
R PrcS	4	52	−4	16
L insula	13	−36	−15	19
R insula	13	45	−13	17
L STG	22	−52	−15	7
L MTG	39	−47	−62	27
R IPL	40	55	−30	23
L precuneus	31	−11	−43	35
L posterior cingulate	31	−9	−43	36
Interaction				
R anterior cingulate	32	5	38	13
R medial FG	9	5	53	21
L insula	13	−43	−8	−5
L STG	22	−56	−33	8
L precuneus	31	−7	−50	30
L posterior cingulate	31	−12	−55	22

Significant contrasts (whole brain random-effects analysis; q(FDR) < 0.05) for the late encoding predictor (4–6 s) are shown. WM-selective = regions showing an effect of WM load only (load 3 vs. load 1, $t = 2.20$); Attention-selective = regions showing an effect of attentional demand only (DS vs. ES, $t = 2.25$); Common deactivation = regions showing an effect of WM load and attentional demand; Interaction: load 3 vs. load 1 × DS vs. ES ($t = 2.15$). Talairach coordinates [x, y, z (in millimeters)] of the activation maxima are shown. BA = Brodmann Area; FG = frontal gyrus; IFG = inferior frontal gyrus; IPL = inferior parietal lobule; MTG = middle temporal gyrus; PrcS = precentral sulcus; SFG = superior frontal gyrus; SMG = supramarginal gyrus; STG = superior temporal gyrus.

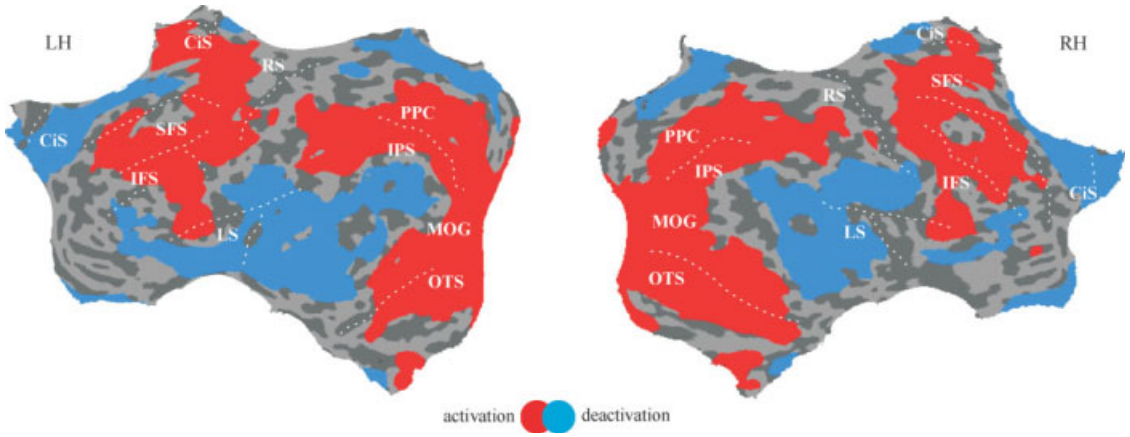

Figure 2.

Activations (red) and deactivations (blue) compared to the baseline revealed by the late encoding predictors (4–6 s after stimulus onset). Group data are projected on the flattened surface reconstruction of the MNI template brain (courtesy of the Montreal Neurological Institute). Activations and deactivations are those exceeding a whole-brain false discovery rate threshold of $q(\text{FDR}) < 0.05$. (LH: left hemisphere, RH: right hemisphere). CiS: cingulate sulcus, IFS: inferior frontal sulcus, IPS: inferior parietal sulcus, LS: lateral sulcus, MOG: middle occipital gyrus, OTS: occipito-temporal sulcus, PPC: posterior parietal cortex, RS: rolandic sulcus, SFS: superior frontal sulcus.

RESULTS

Common and Selective Patterns of BOLD Deactivation for Visual Attention and WM Encoding

During late encoding (4–6 s after stimulus onset) BOLD activity decreased in comparison to baseline activity in several areas that belong to the DMN (see Fig. 2), bilaterally in the medial parietal cortex (PCC, precuneus), the lateral parietal cortex (angular gyrus, SMG), and the anterolateral temporal cortex including the posterior end of the Sylvian fissure and the superior and middle temporal gyri. Deactivated regions in the frontal cortex included the medial frontal gyrus, the ACC, and parts of the lateral superior frontal and inferior frontal gyri. In contrast, increases in BOLD activity were found at lateral fronto-parietal sites [Mayer et al., 2007b] that largely conform to those reported in earlier studies on WM and attention [Corbetta et al., 2002; Linden et al., 2003; Munk et al., 2002; Pessoa and Ungerleider, 2004; Pollmann and von Cramon, 2000].

To test the default mode theory we first compared common and selective patterns of BOLD deactivation in response to the demands on visual attention and WM during late encoding (4–6 s after stimulus onset). As shown in Figure 3, a subset of the task-induced deactivations was modulated by the demands on attention, WM load, or both. Regions that showed stronger deactivations for both DS compared to ES conditions and for WM Load 3 compared to Load 1 included the left PCC and precuneus, the left superior and middle temporal gyri, and bilateral insula extending into the caudal ends of the precentral and postcentral gyri. Time course analyses of these regions indicated that the BOLD response additively decreased from baseline as a consequence of an increase in the demands on WM encoding and attention. Thus, the BOLD response decreased from WM Load 1 to WM Load 3 and from ES to DS, with the strongest decrease in Load 3/DS, the condition with high demands on both attention and WM (Fig. 3, green, Table I). The additivity of the effects of WM load and search difficulty was supported by the lack of a significant interaction between the two factors in most of these overlap regions. A significant interaction effect between WM load and search difficulty emerged only in the left posterior parietal cortex (precuneus, PCC).

Areas suppressed by high attentional demand but not WM load were found in the left lateral PFC (superior and inferior frontal gyri) and bilaterally in the medial frontal cortex (medial frontal gyrus, ACC, paracentral lobule). Posterior regions included the left middle and bilateral superior temporal gyri, the left angular gyrus, and posterior parts of the right insula. Amongst the subcortical regions, the globus pallidus was suppressed bilaterally. These regions showed stronger BOLD deactivation in the DS vs. the ES irrespective of WM load (Fig. 3, yellow, Table I).

In contrast, regions that were suppressed by high WM load but not attentional demand appeared mainly in the right hemisphere and included the medial-parietal cortex (PCC, precuneus), the SMG, and temporal regions. Frontal regions included the anterior medial frontal gyrus bilaterally, the right ACC, and the right inferior frontal gyrus. BOLD deactivation in these regions increased to the same degree from WM Load 1 to Load 3, irrespective of search difficulty (Fig. 3, blue, Table I). Overall, deactivation in

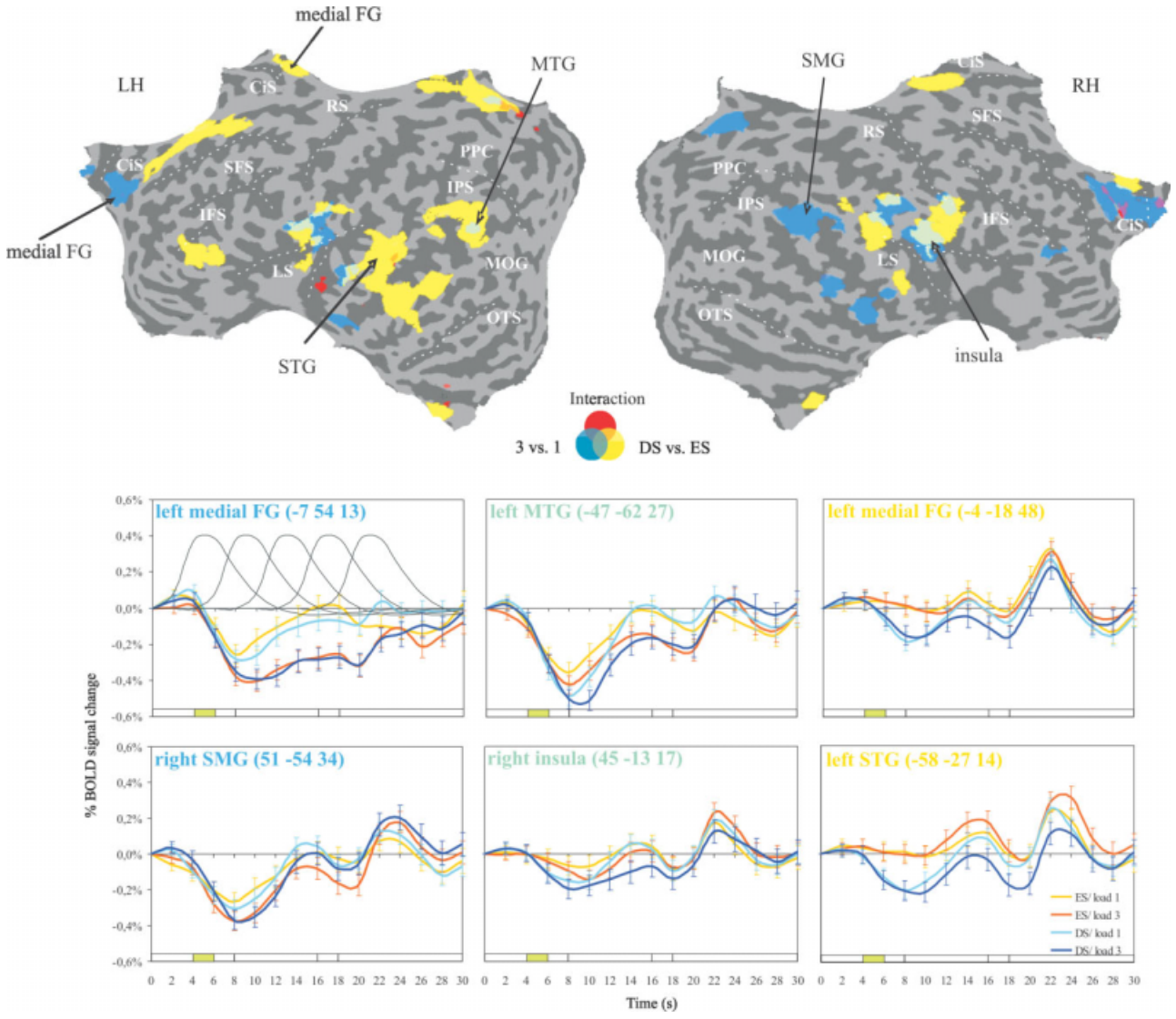

Figure 3.

Deactivations in the four experimental conditions during late encoding (4–6 s). Statistical maps of the contrasts DS vs. ES (yellow), WM Load 3 vs. 1 (blue, green: overlap), and the interaction of search difficulty × WM load (red) are shown. Averaged time courses of the BOLD response are given for selected ROIs together with the predictors modeling the different task phases. Deactivations are those exceeding a whole-brain false discovery rate threshold of $q(\text{FDR}) < 0.05$. DS: difficult search, ES: easy search, FG: frontal gyrus, MTG: middle temporal gyrus, SMG: supramarginal gyrus, STG: superior temporal gyrus, green bar: late encoding predictor.

response to attentional demand appeared to be stronger in the left, and to WM load in the right hemisphere. When modeling BOLD activity in each experimental condition across the whole encoding phase (0–8 s after stimulus onset, Models nos. 1 and 2), we found highly similar results. The only difference appeared in the left superior/middle temporal gyri, a region that was modulated not only by attentional demand but also WM load in the additional analyses (Supporting Information Fig. 1B,C). Modeling each experimental condition across the whole trial resulted in a similar WM load effect whereas the attention effect and the interaction between WM load and attentional demand did not reach significance (Supporting Information Fig. 1D). These findings indicate that in the present task BOLD deactivation was differentially modulated with respect to the task component (attentional demand, WM load) and task phase (encoding, delay, retrieval).

The specificity of regional differences in deactivation related to WM load and attentional demand was further

TABLE II. Results from the contrast DS1 vs. ES3 during encoding

Brain region	BA	*x*	*y*	*z*	*t*	*P*
WM-selective						
R anterior cingulate	42	6	41	7	3.27	0.001
R medial FG	9	4	47	29	3.16	0.002
R SMG	40	51	−54	34	2.24	0.025
Attention-selective						
L medial FG	6	−4	−18	48	−3.31	0.001
L paracentral lobule	31	−5	−30	47	−3.85	0.000
R paracentral lobule	6	8	−24	46	−2.42	0.015
R insula	13	50	−33	18	−2.24	0.025
L STG	42	−58	−27	14	−2.19	0.029
R STG	22	51	−10	9	−2.32	0.020
L angular gyrus	39	−41	−65	36	−2.17	0.029
L globus pallidus		−16	−10	−7	−4.86	0.000
R globus pallidus		25	−12	−7	−3.23	0.001
Common deactivation						
R PrcS	4	52	−4	16	−1.51	0.131
L insula	13	−36	−15	19	−1.07	0.283
R insula	13	45	−13	17	−0.89	0.373
L STG	22	−52	−15	7	−1.73	0.082
L MTG	39	−47	−62	27	−1.84	0.066
R IPL	40	55	−30	23	−1.22	0.223
L precuneus	31	−11	−43	35	−1.20	0.230
L posterior cingulate	31	−9	−43	36	−1.79	0.074

The contrast DS1 vs. ES3 was calculated for those regions that showed a significant effect of attentional demand, WM load or both in the whole-brain analyses (see Table I). For WM-selective and attention-selective regions only significant results are shown. In all other regions the contrast was not significant (all *P* values > 0.16). Positive *T*-values: stronger activation for WM load vs. attentional demand; negative *T*-values: stronger activation for attentional demand vs. WM load. Talairach coordinates [*x*, *y*, *z* (in millimeters)] are shown. BA = Brodmann Area; FG = frontal gyrus; IPL = inferior parietal lobule; MTG = middle temporal gyrus; PrcS = precentral sulcus; SMG = supramarginal gyrus; STG = superior temporal gyrus.

tested by contrasting the effects of search difficulty and WM load. ROI analyses confirmed that deactivation in the right ACC, medial frontal gyrus, and SMG was stronger in response to WM load than attentional demand. In contrast, the effect of attentional demand was found to be significantly greater than the effect of WM load in the majority of regions associated with an effect of attention in the whole-brain analysis. Importantly, regions of common deactivation for WM load and attentional demand did not show significant differences (Table II). These results provide supporting evidence that the deactivations related to WM load and attentional demand were indeed to a high degree spatially distinct.

The specificity of regional differences in deactivation was also tested within regions of the DMN as defined in the literature [Shulman et al., 1997] (Table III). A stronger effect of attentional demand compared to WM load was found in two left parietal ROIs whereas the opposite effect with stronger deactivation in response to WM load vs. attentional demand appeared in the right medial frontal gyrus. Deactivation in the right angular gyrus was modulated to the same degree by WM load and attentional demand as indicated by the lack of a significant difference between the two task components. Additional regions reported by Shulman et al., [1997] were associated with patterns of deactivation independent of the specific task demands (L8/9, L9, L10, M10, M32, L20) with the exception of four ROIs showing an increase in activation rather than a decrease (amygdala, L10/47, L lateral 8, L40). Taken together, these analyses demonstrate a segregation of areas within the DMN where the amplitude of BOLD deactivation was not differentially modulated by the specific task demands and areas that were selectively responsive to either WM load or attentional demand. These findings indicate that task-induced deactivations in some but not all default regions depend on the specific characteristics of the attention and WM components of the task.

Functional Connectivity for Attention and WM Encoding

The task-dependence of deactivation was further investigated by comparing the functional connectivity between regions selectively responsive to WM load and attention

TABLE III. Default mode regions showing differential activation for attentional demand and WM load during encoding

				Attentional demand		WM load		Attentional demand vs. WM load	
Brain region	*x*	*y*	*z*	*t*	*P*	*t*	*P*	*t*	*P*
M 31/7	−5	−49	40	−4.11	0.000	−0.46	0.65	−2.57	0.01
L 39/19	−45	−67	36	−4.38	0.000	−0.77	0.44	−2.54	0.01
R 8/9	5	49	36	0.21	0.84	−3.26	0.001	2.45	0.01
R 40	45	−57	34	−2.71	0.01	−2.89	0.004	0.13	0.90

ROIs were based on the coordinates reported by Shulman et al. [1997]. Results are shown only for those ROIs where significant contrasts for the late encoding predictor (4–6 s) were found (all other *P*-values > 0.10). Attentional demand: (DS1 + DS3) – (ES1 + ES3); WM load: (ES3 + DS3) – (ES1 + DS1); Attentional demand vs. WM load: DS1 vs. ES3.

and other parts of the brain. Based on the multisubject GLM two ROIs were defined as reference regions: the right SMG (deactivated for WM load) and the left SFG (deactivated for attention). The instantaneous influence between these reference regions and other parts of the brain and the difference map are shown in Figure 4. Two observations are of particular importance to the present investigation. First, strong instantaneous influence appears for both reference regions and other frontal and posterior cortical regions with task-induced deactivation (Fig. 4A,B). Second, the comparison of the instantaneous influence for the left SFG and the right SMG indicates quite distinct patterns of brain connectivity with a frontal-posterior gradient for left SFG and right SMG, respectively. The left inferior frontal gyrus and right medial frontal gyrus showed significantly stronger functional connectivity with the left SFG than the right SMG (Fig. 4C, yellow). Conversely, regions bilateral in the medial parietal cortex (PCC, precuneus, right cuneus), the lateral temporo-parietal cortex (angular gyrus, IPL, right MTG), and the right dorsolateral prefrontal cortex (middle and superior frontal gyri) showed significantly stronger functional connectivity with the right SMG than the left SFG (Fig. 4C, blue). These analyses thus demonstrate temporal coherence of BOLD deactivation across brain regions during task execution with task-specific patterns for visual attention and WM.

BOLD Activation and Deactivation for Visual Attention and WM Encoding

Comparing the patterns of BOLD activation and deactivation in response to increased demands on attention and WM encoding, we found complementary modulating effects of task demand. Notably, the increase in task-induced BOLD deactivation mirrored the observed increases in BOLD activation associated with increased search difficulty and/or WM load, but with smaller amplitudes for deactivations than activations [Fig. 5, see also Mayer et al., 2007b]. Time-course analyses indicated that such complementary effects were not restricted to the encoding phase but also appeared during the delay phase and WM retrieval with higher BOLD activation and deactivation for WM Load 3 vs. 1. Interestingly, regions associated with an increase in the magnitude of BOLD deactivation in response to WM load and attentional demand did not necessarily appear adjacent to those regions that showed a complementary increase in BOLD activation but were distributed across the brain.

DISCUSSION

The repeated observation of task-induced deactivations in the medial prefrontal, the medial posterior parietal, and the lateral temporo-parietal cortices across a wide range of cognitive tasks [Binder et al., 1999; Mazoyer et al., 2001; Shulman et al., 1997] has led to the hypothesis of a default mode of brain function that is suspended during goal-directed behavior [Gusnard and Raichle, 2001; Raichle et al., 2001]. In the current study, we tested this hypothesis by comparing common and selective patterns of BOLD deactivation in response to the demands on visual attention and WM encoding that were independently modulated within one task. The analysis of task-induced deactivation revealed three important findings. First, during the encoding phase of the task areas that typically belong to the DMN were deactivated, and this deactivation was modulated by task demand. Second, the patterns of deactivation in response to attentional demand and WM load overlapped in distributed regions but also showed a considerable degree of selectivity. Third, deactivated regions were functionally connected with task-specific patterns for visual attention and WM.

Deactivations Dissociate Between Visual Attention and WM Encoding

Common patterns of deactivation reflecting an additive increase in deactivation under conditions of joint demand on both processes were localized only in the left posterior cingulate gyrus and precuneus, the left temporal lobe, and bilateral insula extending into the caudal ends of the precentral and postcentral gyri. This finding is consistent with previous studies that used separate tasks and showed that the magnitude of deactivation in similar regions of the DMN is sensitive to the difficulty level of both attention and WM tasks [McKiernan et al., 2003, 2006; Todd et al., 2005; Tomasi et al., 2007]. Thus, task-induced deactivations in these overlap regions occurred independent of the specific task component, which is consistent with the default mode theory. However, the regions of overlap were rather small. Similarly, previous studies demonstrated only a small degree of overlap when comparing deactivation patterns in response to increased attentional demand and WM load [McKiernan et al., 2003, 2006; Tomasi et al., 2007]. For instance, McKiernan et al. [2003, 2006] modulated the demands on target detection, target discrimination, and WM within three separate auditory tasks, and found a common effect of task difficulty only in the left ACC/SFG. In addition, a meta-analysis comparing five different cognitively demanding tasks to resting baselines revealed common increases for rest versus tasks only in dorso-medial prefrontal regions [Wicker et al., 2003]. Finally, the finding by Tomasi et al. [2007] that some default mode regions activated during the visual attention task but deactivated during the WM task also challenges the generality of task-independent deactivations. The small degree of overlap observed in the present study should not be due to a lack of sensitivity of the task manipulations because several other regions within the DMN showed significantly stronger deactivation for either high vs. low attentional demand (the left lateral and medial PFC, the left lateral temporal cortex) or WM load (the right medial-parietal and lateral temporo-parietal cortex, the right lateral and medial PFC). This selectivity in location strongly suggests that these

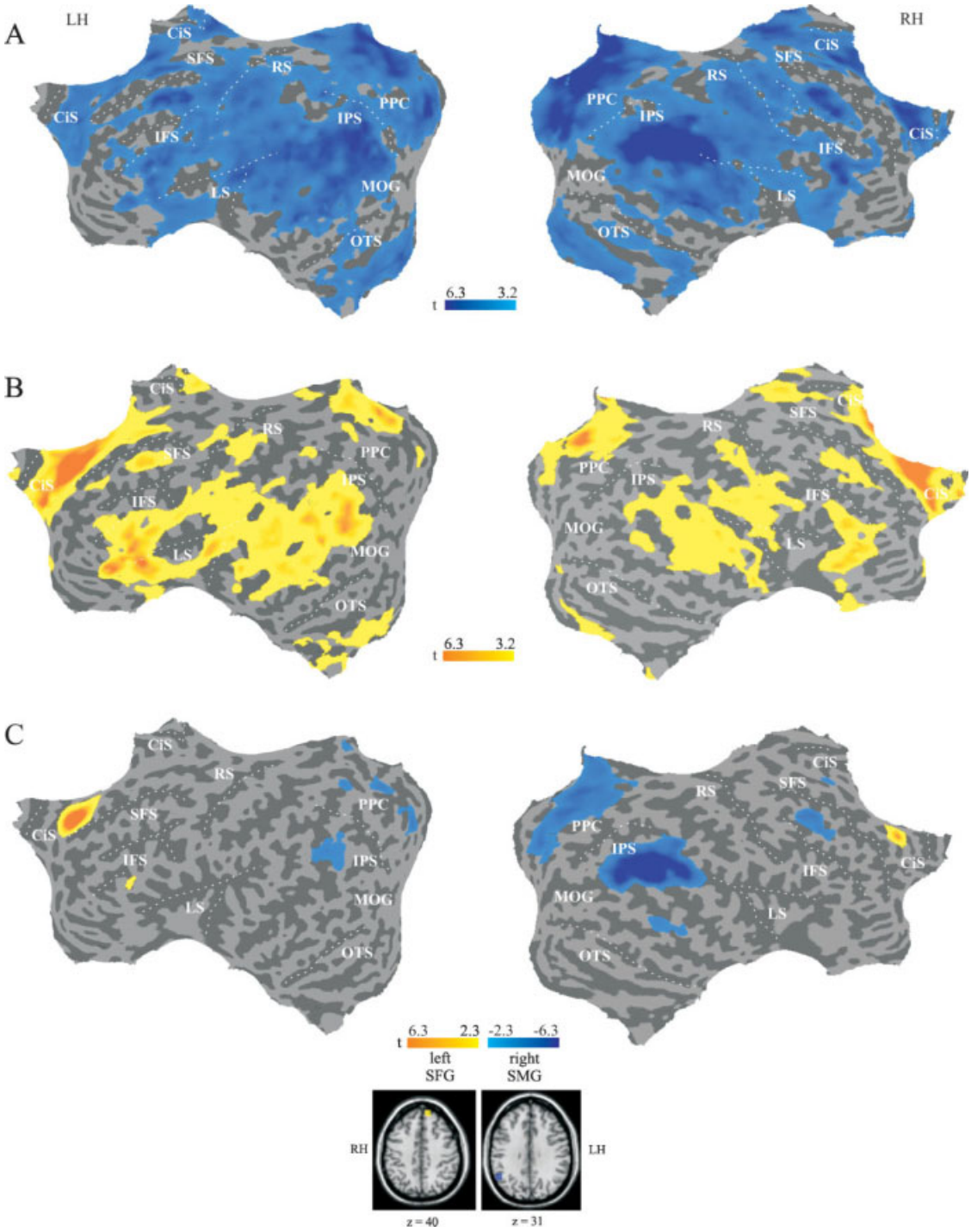

Figure 4.

Functional connectivity maps. (**A**) Instantaneous influence between parts of the brain and right SMG, $P < 0.01$, corrected. (**B**) Instantaneous influence between parts of the brain and left SFG, $P < 0.01$, corrected. (**C**) Difference maps for instantaneous influence between parts of the brain and left SFG vs. right SMG, $P < 0.05$, corrected. Yellow indicates regions showing stronger functional connectivity with the left SFG vs. right SMG. Blue indicates regions showing stronger functional connectivity with the right SMG vs. left SFG. The two reference regions are shown in the transversal slices.

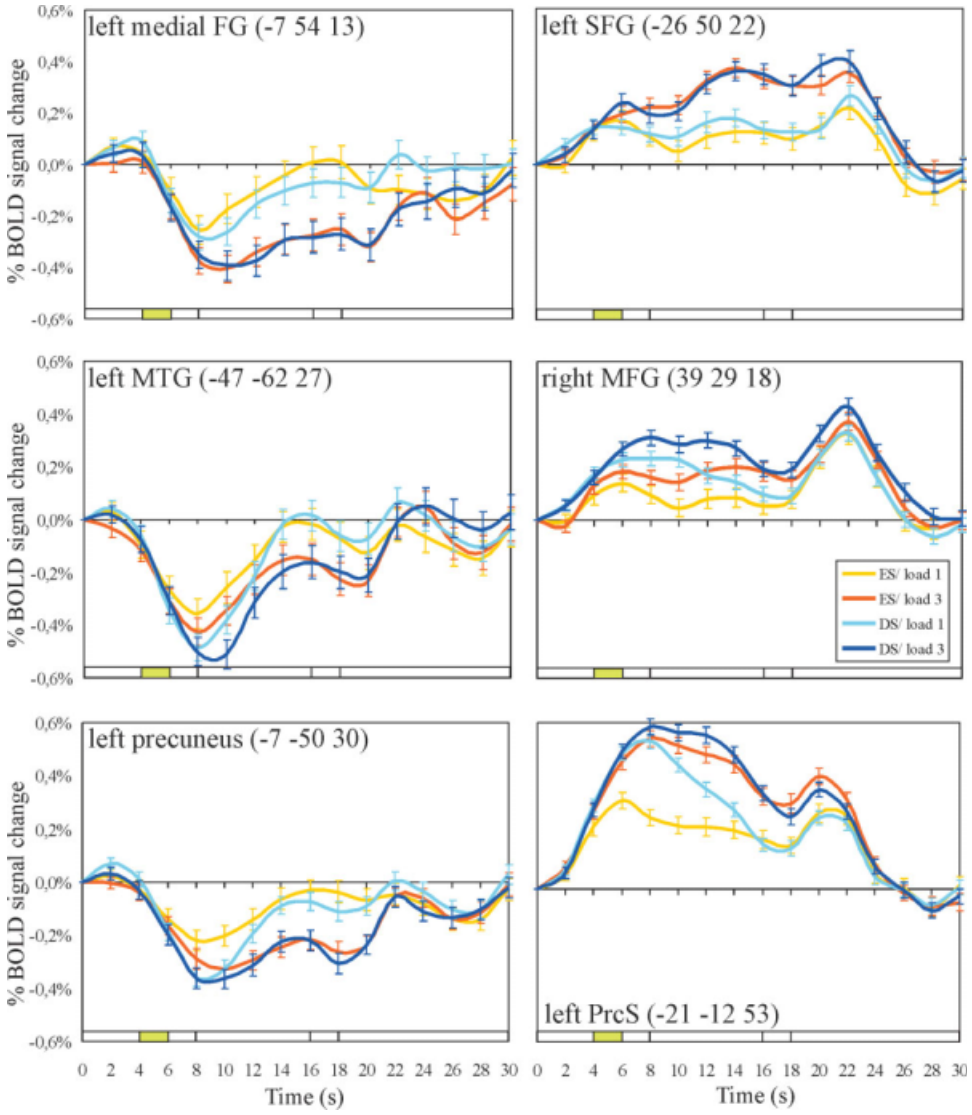

Figure 5.

Deactivations compared with activations in the four experimental conditions. Averaged time courses from selected ROIs associated with significant decreases (left panel) or increases (right panel) from baseline during late encoding (4–6 s) are shown. FG: frontal gyrus, MFG: middle frontal gyrus, MTG: middle temporal gyrus, PrcS: precentral sulcus, SFG: superior frontal gyrus.

decreases in activation depend on the characteristics of the attention and WM task components, a finding that is not explained by the default mode theory. Task-dependent decreases have been most often found in sensory cortices associated with different task modalities. Thus, deactivation of the visual cortices occurs during auditory stimulation whereas auditory cortices are deactivated during visual stimulation [Amedi et al., 2005; Laurienti et al., 2002; Lewis et al., 2000; McKiernan, 2003, 2006]. The present study demonstrates that task-dependent deactivations are not restricted to the sensory cortex but can also occur within the set of brain regions commonly associated with the default mode of brain function [Gusnard and Raichle, 2001; Raichle et al., 2001]. Therefore, we suggest that the classical DMN does not represent a functionally homogeneous state. Rather, the present findings illustrate that parts of this network are functionally fractionated with different contributions to visual attention and WM.

Functional Connectivity Dissociates Between Visual Attention and WM Encoding

The analysis of functional connectivity has become a prominent approach in the study of the DMN in the

resting state [Biswal et al., 1995; Fox et al., 2005; Fransson, 2005; Greicius et al., 2003; Laufs et al., 2003]. These studies have demonstrated that nodes of the DMN are functionally connected at rest supporting the notion of a common function. However, functional connectivity between regions of the DMN has also been observed during the execution of a WM task [Hampson et al., 2006]. Thus, inconsistent with the default mode hypothesis, interactions between component regions of the default mode do not necessarily diminish during cognitive performance. Similarly, our GCM analyses revealed strong functional connectivity between regions of task-induced deactivation during WM encoding. Moreover, we observed differential patterns of brain connectivity for regions that selectively deactivated in response to either high attentional demand or WM load. Our GCM analyses did not aim at defining the DMN because it is usually described in terms of correlations in spontaneous BOLD activity at rest. Yet it is worth noting that analyses of resting state functional connectivity also provided evidence for anatomically distinct networks [Cohen et al., 2008; van de Ven et al., 2004]. Although the comparability of different measures of functional connectivity is limited—for instance, GCM does not consider specific frequencies of the signal fluctuations—the GCM results substantially support the finding of task-specificity by showing temporal coherence of task-specific deactivation patterns in different regions. These findings again point to a functional fractionation of the DMN.

Interpreting Task-Specific Deactivations

It has been suggested that task-induced deactivation reflects the reallocation of cognitive resources from task-irrelevant processes that occur during the conscious resting state to task-relevant processes required during the execution of an active task [Gusnard and Raichle, 2001; Shulman et al., 1997]. Consistent with this notion, the magnitude of task-induced deactivation increases with increased task difficulty [McKiernan et al., 2003, 2006; Singh and Fawcett, 2008; Todd et al., 2005; Tomasi et al., 2007]. However, if task-irrelevant mental processes compete with task processes for cognitive resources and thus result in suppression of a common network under conditions of increased cognitive demand, we would expect an additive increase in BOLD deactivation under simultaneous attention and WM demands with the highest increase in the most demanding condition (DS/Load 3) within the set of deactivated regions. In contrast, our results revealed a considerable degree of selectivity in the patterns of deactivation in response to high attentional demand and WM load. Thus, it does not appear that all task-induced deactivations result from the competition for general processing resources required during an active task and during passive internal processing. This only seems to be the case for the subset of DMN areas that showed nontask selective suppression (the green areas in Fig. 3, common activation in Table I), which we may tentatively term the "core DMN."

The alternative explanation, and the one favored by us, would be that at least some of the task-dependent deactivations of the extended DMN reflect cognitive processes necessary for successful performance of the task at hand. For instance, deactivations in the right SMG have been associated with a filtering mechanism that operates during both active tasks and resting states and aids WM [Shulman et al., 2007; Todd et al., 2005]. Moreover, the finding that performance in a WM task is positively correlated to functional connectivity in the DMN during task execution [Hampson et al., 2006] strongly supports the hypothesis of functional significance of task-induced deactivations. In the present study deactivation-behavior relationships were not assessed due to the lack of a direct behavioral indicator of the process of WM encoding. Although the present study succeeds in demonstrating that task-induced deactivations are largely dependent on the characteristics of the task at hand, future research is needed to determine their functional importance and elucidate the specific processes that may facilitate cognitive performance during attention and WM tasks.

Finally, the physiological mechanisms underpinning task-induced BOLD deactivation are still unclear, thus leaving possible explanations in terms of cognitive processing rather speculative. One hypothesis for task-specific deactivations proposes a blood-stealing effect [Devor et al., 2005; Harel et al., 2002], i.e. the local shunting of cerebral blood flow to areas that are active during the attention and WM components of the task from adjacent areas. However, in the present study deactivation was observed at great distance and across different vascular distributions from the activated brain regions. For instance, activations in response to attentional demand appeared to be stronger in the right and to WM load in the left hemisphere. In contrast, deactivation in response to attentional demand appeared to be stronger in the left and to WM load in the right hemisphere. Thus, although a hemodynamic component cannot be completely ruled out, an explanation of the noted deactivation in terms of neural processing seems likely. Evidence for a neuronal origin of the negative BOLD signal implying a decrease in the firing patterns and synaptic activity of neurons has been provided at least for the visual cortex [Pasley et al., 2007; Shmuel et al., 2002, 2006]. Based on the similarities in the time courses of the positive and negative BOLD responses, e.g. an increase in the amplitude of both responses with increasing stimulus contrast, these studies also suggest a tight coupling between task-induced activations and deactivations in neighboring regions. This coupling might well explain the present finding that the time course of the BOLD deactivation in response to search difficulty and/or WM mirrored qualitatively that of the BOLD activation in distributed regions across the brain. Overall, the amplitude of the negative BOLD responses was considerably smaller than that of the positive BOLD responses, a finding that is consistent

with previous reports [Shmuel et al., 2002, 2006]. Based on the coupling of positive and negative BOLD responses it has been suggested that lateral suppression from the activated regions possibly mediated by inhibitory local or long-range feedback connections from higher visual areas [Angelucci et al., 2002; Shmuel et al., 2002] might account for the reduction in neuronal activity. Furthermore, a reduction in the afferent input from the lateral geniculate nucleus or higher visual areas to the deactivated regions has been discussed [Shmuel et al., 2002]. In the somatosensory system, negative BOLD has been related to the active inhibition of somatosensory cortex by feedforward connections that are triggered by thalamocortcial input [Blankenburg et al., 2003]. Along these lines, it is interesting to note that long-range inhibitory interactions might well exist as there is evidence for suppressive influences that operate between remote but interconnected areas of the human brain even across hemispheres [Ruff et al., 2006, 2008; Sack et al., 2005]. Therefore, a reasonable explanation for the attention- and WM-selective patterns of deactivation observed in the present study is that they originate from inhibitory projections from task-relevant activated regions.

CONCLUSION

Although the exact mechanisms that create the robust deactivation remain to be determined, the finding that task-induced deactivations in WM and attention tasks rely on both the demands on cognitive processing and the characteristics of the specific task illustrates that task-induced deactivation may carry important information that should not be neglected when studying brain function with fMRI. Future studies need to consider differences in deactivations across tasks and investigate their relevance for individual task performance. We would predict that they will replicate the present finding of a task-general "core" DMN, comprising amongst other areas the posterior cingulate and insula bilaterally, and task-specific deactivations in an extended network that varies with the task at hand.

ACKNOWLEDGMENTS

The authors thank Amanda Kaas for advice on data analysis and Robert Bittner for helpful discussions. FMRI was performed at the Frankfurt Brain Imaging Center.

REFERENCES

Amedi A, Malach R, Pascual-Leone A (2005): Negative BOLD differentiates visual imagery and perception. Neuron 48:859–872.

Angelucci A, Levitt JB, Walton EJS, Hupé JM, Bullier J, Lund JS (2002): Circuits for local and global signal integration in primary visual cortex. J Neurosci 22:8633–8646.

Bar M, Aminoff E, Mason M, Fenske M (2007): The units of thought. Hippocampus 17:420–428.

Binder JR, Frost JA, Hammeke TA, Bellgowan PSF, Rao SM, Cox RW (1999): Conceptual processing during the conscious resting state. A functional MRI study. J Cogn Neurosci 11:80–95.

Biswal B, Yetkin FZ, Haughton VM, Hyde JS (1995): Functional connectivity in the motor cortex of resting human brain using echo-planar MRI. Magn Reson Med 34:537–541.

Blankenburg F, Taskin B, Ruben J, Moosmann M, Ritter P, Curio G, Villringer A (2003): Imperceptible stimuli and sensory processing impediment. Science 299:1864.

Cohen AL, Fair DA, Dosenbach NUF, Miezin FM, Dierker D, Van Essen DC, Schlaggar BL, Petersen SE (2008): Defining functional areas in individual human brains using resting functional connectivity MRI. NeuroImage 41:45–57.

Corbetta M, Kincade JM, Shulman GL (2002): Neural systems for visual orienting and their relationships to spatial working memory. J Cogn Neurosci 14:508–523.

Devor A, Ulbert I, Dunn A, Narayanan S, Jones S, Andermann M, Boas D, Dale A (2005): Coupling of the cortical hemodynamic response to cortical and thalamic neuronal activity. Proc Natl Acad Sci USA 102:3822–3827.

Forman SD, Cohen JD, Fitzgerald M, Eddy WF, Mintun MA, Noll DC (1995): Improved assessment of significant activation in functional magnetic resonance imaging (fMRI): Use of a cluster-size threshold. Magn Reson Med 33:636–647.

Fox MD, Snyder AZ, Vincent JL, Corbetta M, Van Essen DC, Raichle ME (2005): The human brain is intrinsically organized into dynamic, anticorrelated functional networks. Proc Natl Acad Sci USA 102:9673–9678.

Fransson P (2005): How default is the default mode of brain function? Further evidence from intrinsic BOLD signal fluctuations. Hum Brain Mapp 26:15–29.

Friston KJ, Fletcher P, Josephs O, Holmes A, Rugg MD, Turner R (1998): Event-related fMRI: Characterizing differential responses. NeuroImage 7:30–40.

Genovese C, Lazar N, Nichols T (2002): Thresholding of statistical maps in functional neuroimaging using the false discovery. NeuroImage 15:870–878.

Goebel R, Roebroeck A, Kim DS, Formisano E (2003): Investigating directed cortical interactions in time-resolved fMRI data using vector autoregressive modeling and Granger causality mapping. Magn Reson Imaging 21:1251–1261.

Greicius MD, Krasnow B, Reiss AL, Menon V (2003): Functional connectivity in the resting brain: A network analysis of the default mode hypothesis. Proc Natl Acad Sci USA 100:253–258.

Gusnard DB, Raichle ME (2001): Searching for a baseline: Functional imaging and the resting human brain. Nat Rev Neurosci 2:685–694.

Hampson M, Driesen NR, Skudlarski P, Gore JC, Constable RT (2006): Brain connectivity related to working memory performance. J Neurosci 26:13338–13343.

Harel N, Lee SP, Nagaoka T, Kim DS, Kim SG (2002): Origin of negative blood oxygenation level-dependent fMRI signals. J Cereb Blood Flow Metab 22:908–917.

Laufs H, Krakow K, Sterzer P, Eger E, Beyerle A, Salek-Haddadi A, Kleinschmidt A (2003): Electroencephalographic signatures of attentional and cognitive default modes in spontaneous brain activity fluctuations at rest. Proc Natl Acad Sci USA 100:11053–11058.

Laurienti PJ, Burdette JH, Wallace MT, Yen YF, Field AS, Stein BE (2002): Deactivation of sensory-specific cortex by cross-modal stimuli. J Cogn Neurosci 14:420–429.

Lewis JW, Beauchamp MS, DeYoe EA (2000): A comparison of visual and auditory motion processing in human cerebral cortex. Cereb Cortex 10:873–888.

Linden DEJ, Bittner RA, Muckli L, Waltz JA, Kriegeskorte N, Goebel R, Singer W, Munk MHJ (2003): Cortical capacity constraints for visual working memory: Dissociation of fMRI load effects in a fronto-parietal network. NeuroImage 20:1518–1530.

Mason MF, Norton MJ, Van Horn JD, Wegner DM, Grafton ST, Macrae CN (2007): Wandering minds: The default network and stimulus-independent thought. Science 315:393–395.

Mayer JS, Bittner R, Linden DEJ, Nikolić D (2007a): Attentional demand influences strategies for encoding into visual working memory. Adv Cogn Psychol 3:429–448.

Mayer JS, Bittner RA, Nikolić D, Bledowski C, Goebel R, Linden DEJ (2007b): Common neural substrates for visual working memory and attention. NeuroImage 36:441–453.

Mazoyer B, Zago L, Mellet E, Bricogne S, Etard O, Houdé O, Crivello F, Joliot M, Petit L, Tzourio-Mazoyer N (2001): Cortical networks for working memory and executive functions sustain the conscious resting state in man. Brain Res Bull 54:287–298.

McKiernan KA, Kaufman JN, Kucera-Thompson J, Binder JR (2003): A parametric manipulation of factors affecting task-induced deactivation in functional neuroimaging. J Cogn Neurosci 15:394–408.

McKiernan KA, D'Angelo BR, Kaufman JN, Binder JR (2006): Interrupting the "stream of consciousness": An fMRI investigation. NeuroImage 29:1185–1191.

Munk MH, Linden DEJ, Muckli L, Lanfermann H, Zanella FE, Singer W, Goebel R (2002): Distributed cortical systems in visual short-term memory revealed by event-related functional magnetic resonance imaging. Cereb Cortex 12:866–876.

Pasley BN, Inglis BA, Freeman RD (2007): Analysis of oxygen metabolism implies a neural origin for the negative BOLD response in human visual cortex. NeuroImage 36:269–276.

Pessoa L, Ungerleider LG (2004): Top-down mechanisms for working memory and attentional processes. In: Gazzaniga MS, editor. The New Cognitive Neurosciences. Cambridge, MA: MIT Press. pp 919–930.

Pollmann S, von Cramon DY (2000): Object working memory and visuospatial processing: Functional neuroanatomy analyzed by event-related fMRI. Exp Brain Res 133:12–22.

Raichle ME, MacLeod AM, Snyder AZ, Powers WJ, Gusnard DA, Shulman GL (2001): A default mode of brain function. Proc Natl Acad Sci USA 98:676–682.

Roebroeck A, Formisano E, Goebel R (2005): Mapping directed influence over the brain using Granger causality and fMRI. NeuroImage 25:230–242.

Ruff CC, Blankenburg F, Bjoertomt O, Bestmann S, Freeman E, Haynes JN, Rees G, Josephs O, Deichmann R, Driver J (2006): Concurrent TMS-fMRI and psychophysics reveal frontal influences on human retinotopic visual cortex. Curr Biol 16:1479–1488.

Ruff CC, Bestmann S, Blankenburg F, Bjoertomt O, Josephs O, Weiskopf N, Deichmann R, Driver J (2008): Distinct causal influences of parietal versus frontal areas on human visual cortex: Evidence from concurrent TMS-fMRI. Cereb Cortex 18:817–827.

Sack AT, Camprodon JA, Pascual-Leone A, Goebel R (2005): The dynamics of interhemispheric compensatory processes in mental imagery. Science 308:702–704.

Schridde U, Khubchandani M, Motelow JE, Sanganahalli BG, Hyder F, Blumenfeld H (2008): Negative BOLD with large increases in neuronal activity. Cereb Cortex 18:1814–1827.

Shmuel A, Yacoub E, Pfeuffer J, Van de Moortele PF, Adriany G, Hu X, Ugurbil K (2002): Sustained negative BOLD, blood flow and oxygen consumption response and its coupling to the positive response in the human brain. Neuron 36:1195–1210.

Shmuel A, Augath M, Oeltermann A, Logothetis NK (2006): Negative functional MRI response correlates with decreases in neuronal activity in monkey visual area V1. Nat Neurosci 9:569–577.

Shulman GL, Fiez JA, Corbetta M, Buckner RL, Miezin FM, Raichle ME, Petersen SE (1997): Common blood flow changes across visual tasks: II. Decreases in cerebral cortex. J Cogn Neurosci 9:648–663.

Shulman GL, McAvoy MP, Cowan MC, Astafiev SV, Tansy AP, d'Avossa G, Corbetta M (2003): Quantitative analysis of attention and detection signals during visual search. J Neurophysiol 90:3384–3397.

Shulman GL, Astafiev SV, McAvoy MP, d'Avossa G, Corbetta M (2007): Right TPJ deactivation during visual search: Functional significance and support for a filter hypothesis. Cereb Cortex 17:2625–2633.

Singh KD, Fawcett IP (2008): Transient and linearly graded deactivation of the human default-mode network by a visual detection task. NeuroImage 41:100–112.

Todd JJ, Fougnie D, Marois R (2005): Visual short-term memory load suppresses temporo-parietal junction activity and induces inattentional blindness. Psychol Sci 16:965–972.

Tomasi D, Ernst T, Caparelli EC, Chang L (2007): Common deactivation patterns during working memory and visual attention tasks: An intra-subject fMRI study at 4 Tesla. Hum Brain Mapp 27:694–705.

van de Ven VG, Formisano E, Prvulovic D, Roeder CH, Linden DE (2004): Functional connectivity as revealed by spatial independent component analysis of fMRI measurements during rest. Hum Brain Mapp 22:165–178.

Wicker B, Ruby P, Royet JP, Fonlupt P (2003): A relation between rest and the self in the brain? Brain Res Brain Res Rev 43:224–230.

Zarahn E, Aguirre G, D'Esposito M (1997): A trial-based experimental design for fMRI. NeuroImage 6:122–138.